The first lidar observations of the nighttime sodium layer at low latitudes Gadanki (13.5°N, 79.2°E), India

Y. Bhavani Kumar[1], P. Vishnu Prasanth[2], D. Narayana Rao[1], M. Sundara Murthy[2], and M. Krishnaiah[2]

[1]*National Atmospheric Research Laboratory (NARL), P.B No 123, Tirupati 517 502, India*
[2]*S.V.University, Tirupati-517 502, India*

We report on the first lidar observations of the nighttime mesospheric sodium layer from Gadanki (13.5°N, 79.2°E) site in India. The lidar measurements of upper atmospheric sodium made on 6 nights between the 10 and 16 January 2005 are presented in this paper. The Gadanki lidar uses a Nd:YAG pumped dye laser, tuned to the sodium D2 line (589.0 nm), as a transmitter. Using the system, sodium number density profiles have been obtained with a vertical resolution of 300 m, a time sampling of 120 s. During the initial six nights of observation, the peak sodium concentration is found at a height of 95 km, and the top side scale height is usually about 2 km. On three occasions, a secondary peak was observed at heights between 87 and 92 km. Measurements at Gadanki site indicate that the mean sodium abundances appear to decrease after sunset and increase before sunrise. The average nocturnal columnar abundances were in the range 2–8.9×10^9 cm^{-2}. The nightly mean centroid heights range between 92.9 and 95.2 km and the rms widths vary between 4.3 and 4.9 km. On some nights, wave like structures in the sodium layer were observed with wavelength of about 3 km and downward phase velocities of about 1 km/hr. Four sporadic layers were observed during the initial 54 h of observation. The formation and decay of an intense sporadic sodium layer was observed on the night of 11 January 2005. The layer was found to develop between 93 and 90 km altitude and appear between 0230 and 0430 LT.

Key words: Resonance lidar, mesospheric sodium, sporadic sodium, mesospheric chemistry, gravity waves, sodium layer.

1. Introduction

It is well known that metallic sodium atoms exist in the neutral state in the upper part of the atmosphere (Slipher, 1929). Ablation of meteorites and comet dusts is believed to be the dominant source for the formation of sodium (Na) and other metal layers in the mesosphere (Bills and Gardner, 1990; Clemesha *et al.,* 1992; Alpers *et al.,* 1993). The mesospheric Na layer generally appears in the altitude range of 80 to 110 km with a peak close to the mesopause where the Na number density is of the order of 10^3 to 10^4 cm^{-3} (Richter *et al.,* 1981).

Since the mesospheric region is difficult to measure, being too low for satellites and too high for balloons and rocket flights are too infrequent, most studies rely on remote-sensing techniques. Over the past three decades, resonance lidar systems have been used to study most of the alkaline metals and dynamics of the mesopause region. The metal layers are useful for remote sensing as they can be excited at specific wavelengths to emit resonance fluorescence. For sodium the resonant wavelength is 589 nm, bright orange in color, which matches the frequency of Na atomic transition from the ground state to the first-excited state. The resonance scatter occurs when the absorbed radiation is re-emitted by the Na atoms. The resonance scattering is one of the most efficient scattering processes in the atmosphere. It is noted that the Rayleigh backscatter cross-section at 589 nm wavelength is about 3×10^{-31} m^2 (Nicolet, 1984), while the Na-resonance cross-section of the D$_2$ line is about 10^{-15}–10^{-16} m^2 (Fricke and von Zahn, 1985). This shows that the Na cross-section is about 15–16 orders of magnitude larger than the Rayleigh or molecular cross-section. Because of this reason, the mesospheric sodium has become the most frequently studied metallic component of the Earth's atmosphere.

Resonance lidar observations of the atmospheric sodium layer have been made by numerous groups at different locations. These studies show that the mesospheric sodium layer is subject to seasonal and shorter term variations, which differ significantly from location to location (Kwon *et al.,* 1988; Clemesha *et al.,* 1992; Kane *et al.,* 1993; Clemesha, 1995; Nagasawa and Abo, 1995; Clemesha *et al.,* 1999; Kane *et al.,* 2001; Yi *et al.,* 2002). The sodium layer is also an excellent tracer of the atmospheric wave motion. Perturbations generated by atmospheric tides and gravity waves have been detected by various workers (Batista *et al.,* 1985; Gardner and Shelton, 1985; Gardner and Voelz, 1987; States and Gardner, 1999).

Much of the information about the mesospheric atomic sodium layer has been obtained from lidar measurements around the globe. However, the measurements in the tropical region are relatively sparse in comparison to those available at mid and high latitudes. Though there are some lidar

Table 1. Main specifications of sodium lidar.

Transmitter	
Pump Laser	
Continuum, USA make Power Lite model 8020	
Repetition rate	20 Hz
Energy (per pulse)	200 mJ max
Laser beam size	8 mm
Beam divergence	0.5 mrad
Pulse width	6 ns
Line width	1 cm^{-1}
Dye Laser	
Continuum, USA make Jaguar Narrow scan model D90DMA	
Tunable range	$330 - 740$ nm
Tuning mechanism	Dual Grating
Dye used	Sulfo Rhodamine B (Kiton Red)
Energy (per pulse)	25 mJ (normal)
Conversion efficiency	20 percent maximum
Grating resolution	2400 lines/mm
Precision	1 pm
Divergence	Set to 1.0 mrad
Line width	0.05 cm^{-1} or 2 picometer
Stability	$0.05 \text{ cm}^{-1} \, {}^{\circ}\text{C}^{-1} \text{ hours}^{-1}$
External beam expander	10 X
(CVI, USA)	
Divergence	$100 \, \mu\text{rad}$
(After beam expander)	
Receiver	
Telescope diameter	750 mm, Newtonian type
Field of View	1.0 mrad
IF filter CW	589.0 nm
IF filter FWHM	1.0 nm
Peak transmission	60 percent
PMT	12 dynode, low dark current (1 nA), not peltier cooled type
PMT	$R3234 - 01$, Head-on type, Hamamatsu, Japan make
Quantum efficiency	8 percent
Gain of PMT	2.5×10^7 units
Data acquisition system	
Type	Single photon counting
Model	EG and G Ortec, MCS-plus
Maximum counting rate	100 MHz
Bin width	$2 \mu s$
Number of bins per pulse	1024

observations of the mesospheric sodium that have been reported from a few low latitude stations such as Mauna Kea, Hawaii (20°N) (Kwon *et al.,* 1988) and Arecibo, Puerto Rico (18°N) (Beatty *et al.,* 1989), Kototabang, Indonesia (0.2°S) (Shibata *et al.,* 2006), however, there no measurements at other lower latitudes. Another important feature of the sodium layer is the event of sporadic sodium, occurrence of sharp sodium densities in short time, whose formation mechanism is still not understood. However, the recent report by Clemesha *et al.* (1998) show that the occurrence rate of sporadic Na layers at a southern hemisphere low latitude site is quite different compared to the northern hemisphere low latitude location (Kwon *et al.,* 1988). Thus, the measurements of mesospheric sodium at the least

probed low latitude sites are important and valuable to understand the latitudinal behavior and dynamics of atmospheric sodium layer.

Recently a resonant-scatter lidar system has been setup at the National Atmospheric Research Laboratory (NARL), Gadanki (13.5°N, 79.2°E; dip 12.5°N, 6.3° magnetic latitude), to study the aeronomy of the mesopause region over this tropical low-latitude site on regular basis. Using the lidar system, we have observed Na layer at altitudes between 80 and 105 km during January 2005 for the first time over the Indian sub-continent and also observed sporadic formation of thin dense layers of sodium during late night hours. In this paper, we present the preliminary observations made during January 2005.
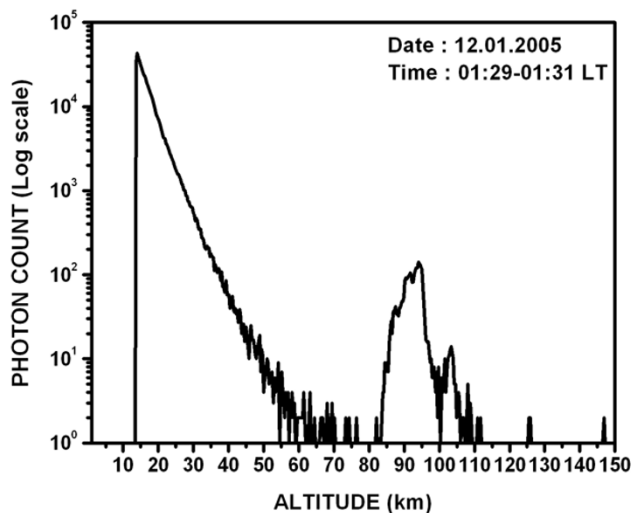
Fig. 1. Photon count profile obtained by integrating the laser returns from 2400 shots.
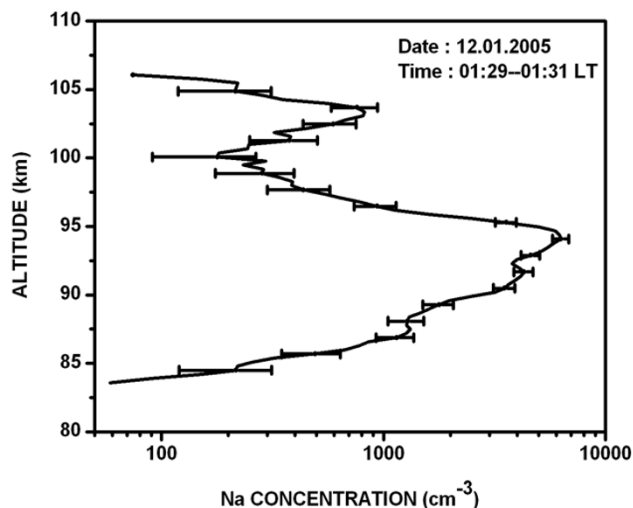

Fig. 2. Height profile of Na number density derived from the photon count profile shown in Fig. 1. The horizontal bars represent statistical error in the retrieved Na number density. The error bars shown are mentioned for the selected measurement points.

2. Equipment setup

A state-of-the art Rayleigh and Mie backscattering lidars (Bhavani Kumar *et al.*, 2000, 2001, 2006) were set up at Gadanki (13.5°N, 79.2°E) in 1998 under the Indo-Japanese collaboration programme. Recently the lidar system was augmented with the capability of probing the mesospheric sodium. The broadband Na lidar system at Gadanki was setup in a mono-static configuration. The power-aperture product of the lidar system was approximately 0.35 W-m^2. The detailed specifications of lidar system are given in Table 1.

The transmitter consists of a tunable pulsed dye laser pumped by a frequency-doubled Nd:YAG-laser. The pulsed dye laser is tuned to the D$_2$ resonant absorption line of Na at a wavelength near 589 nm. The dye laser employs a dual grating system that is controlled by a computer and which enables a rapid selection of transmitted wavelength. The line width of laser is about two picometer. The dye laser is pumped with 200 mJ at 532 nm to get an output pulse energy of 30 mJ at 589 nm. The dye laser uses Kiton Red as laser medium. The laser beam is expanded and transmitted into the atmosphere using a steering mirror. The receiving system uses a 750 mm Newtonian telescope with field optics and an interference filter. We employed photomultiplier tube (PMT) for photon detection. The output pulses of the PMT are amplified by a broadband amplifier and then fed into a PC based photon counting multichannel scalar (MCS). The MCS counts the pulses in successive time bins. Each time bin is set to 2 μs, corresponding to a vertical resolution of 300 m. The photon counts are accumulated for 2400 shots that corresponding to a time resolution of 120 s. A typical photon profile is shown in Fig. 1.

The resonant scattering from the Na layer is clearly seen between 80 and 100 km. The strong photon counts at 30–60 km heights are essentially due to the Rayleigh-scattering from air molecules. A sudden fall in signal counts below 12 km was due to the application of electronic gating to PMT. The observed nonzero count rate at 60–80 km and above 110 km altitude is caused by background noise which includes any light sources other than the emitter light such as airglow emission, starlight, detector dark counts. It may be mentioned here that the background signal returns much above Na layer whose count level was stable and constant over the integration period is utilized in the Na density retrieval. The Na number density profiles are determined with standard computational technique given by Gardner (1989). The computational method involves the processing of photon count data for background noise correction and range normalization. The normalization altitude is usually taken above the background aerosol layer, which means above 30–35 km altitude. From the processed data and by using reference temperature and pressure for January from standard atmosphere model (CIRA 86), we calculated the absolute Na density profiles. However, the presence of sodium layer at mesospheric height causes the differential extinction to the laser beam transmission. Hence, a differential extinction correction is required for the retrieved Na column densities (Fricke and von Zahn, 1985; Simonich and Clemesha, 1983).

Figure 2 shows the retrieved Na number density profile with the differential extinction correction. It has been obtained from the photon count profile shown in Fig. 1. The Na density profiles are obtained with a vertical resolution of 300 m and a time sampling of 120 s. The statistical error in the retrieved Na number density is shown in Fig. 2 as horizontal bars at selected altitudes over the Na number density profile. The detailed system and method of the mesospheric Na number density computation and the statistical error from the NARL sodium lidar is given elsewhere by Bhavani Kumar *et al.* (2007).

3. Results and Discussion

The resonance lidar measurements of mesospheric sodium were made at Gadanki on 6 days between the 10 and 16 January 2005. During most of the measurement, period sky conditions were clear. The time periods over which the lidar was operated are shown in Table 2.

Table 2. Timing details of Na layer measurements at Gadanki site during January, 2005.

Date	Start time	End time	Total duration (hrs)
10 January 2005	22.21	02.27	04.06
11 January 2005	18.47	05.51	11.04
12 January 2005	19.03	05.54	10.51
13 January 2005	19.03	06.00	10.57
15 January 2005	21.15	05.53	08.38
16 January 2005	19.57	05.55	10.58

Parameters such as profile structure, layer properties, wave parameters and formation characteristics of sporadic thin dense layers generally characterize the mesospheric Na layer. The profile structure of mesospheric Na layer shows the distribution of sodium in the layer, top and bottom scale heights and the altitude of peak sodium. The layer parameters such as column abundance (C_o), centroid height (z_o) and rms width (σ_o) provide the structure of the mesospheric sodium layer. Wave parameters inform the details of propagating wave period, velocity and wave number. Characteristics of sporadic formation of thin dense layers of sodium include their time of occurrence, duration, thickness, altitude and maximum density.

3.1 Profile structure

Figure 3 shows the average sodium profile for the entire measurement period. The mean sodium profile starts to appear around 80 km. During the measurement period, only once, we see sodium lower than this but not below 75 km. The layer reaches its peak close to 95 km and then falls to near zero value around 105 km. The peak density value is around 4000 cm^{-3}. The measured profile structure of the sodium layer is very similar to that observed at other locations (Kirchhoff and Clemesha, 1973; Clemesha *et al.*, 1998). Above the peak, the vertical gradient in sodium number density was seen with a smaller scale height, which is about 2 km. Photo-ionisation has been suggested as loss mechanism which produce a steep topside by removing atoms as they diffuse upwards (Hanson and Donaldson, 1967). Above 90 km, the Na layer is controlled by ionic rather than neutral chemistry (Plane, 1991). On the bottom side of the layer, the sodium density falls off less rapidly. However, the sodium profile measured on 10 January 2005 shows an unusually small-scale height, with a steep gradient, on the underside of the sodium number density between the heights of 83 and 85 km. A rapid decrease in the atomic Na number density on the underside of the layer is mainly caused by the corresponding decrease in atomic H and O (Clemesha *et al.*, 1995). With respect to the bottom side of the sodium layer, a number of loss mechanisms for the removal of sodium have been suggested in the literature: these include oxidation, mainly by O_2 and O_3, the formation of cluster ions, and attachment of aerosols particles (Richter and Sechrist, 1979; Hunten, 1981; Kirchoff *et al.*, 1981; Granier *et al.*, 1985; Plane, 1991; Clemesha *et al.*, 1995). The top vertical gradient in sodium density is quite similar to the observations reported by Kirchhoff and Clemesha (1973) at 23°S and Clemesha *et al.* (1998) at 2°S. The centroid height for the mean profile shown in Fig. 3 is
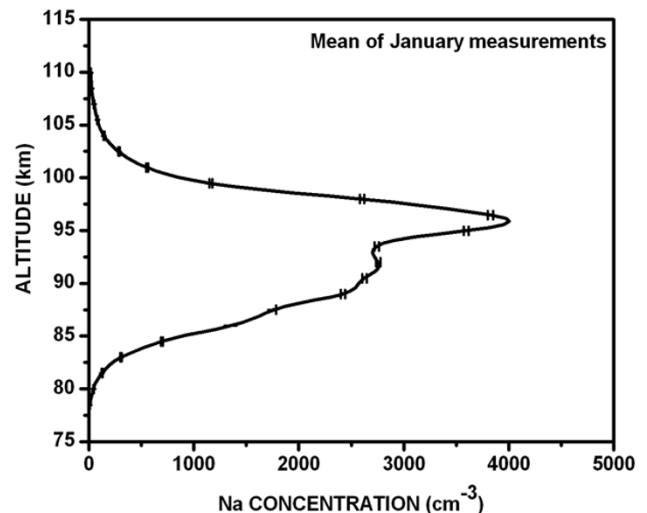

Fig. 3. Mean vertical distribution of the mesospheric sodium measured at Gadanki during January 2005.
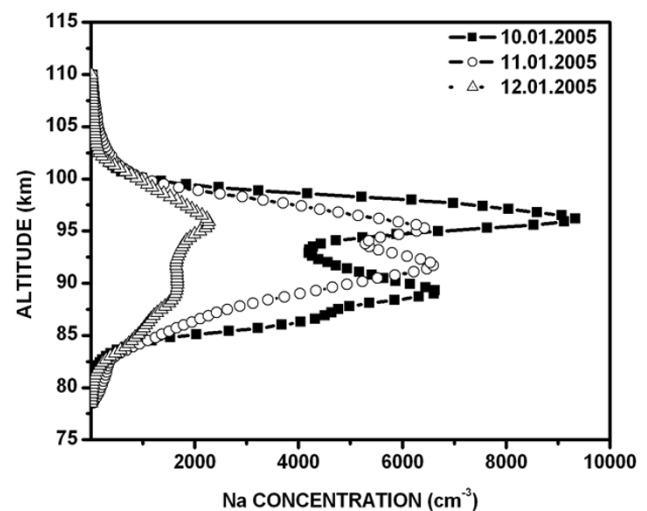

Fig. 4. Mean Na profiles for 10, 11, and 12 January 2005 showing double peaked structure.

93.0 km. This is 900 m above the Sao Jose (23°S) annual mean and 500 m higher to the measured mean at Alcantara (2°S) (Clemesha *et al.,* 1998).

In Fig. 4, we show the average profiles for three consecutive nights 10, 11, 12 January 2006. These profiles show a double peaked structure with primary layer peak at about 95 km. The secondary peak in sodium number density was observed at heights between 87 and 92 km. The mesosphere is a region of complex photochemical and dynamic interaction. The distribution of sodium strongly depends on background distribution of the minor species, such as O_3, O, and H (Clemesha *et al.*, 1995; Xu *et al.*, 2003). It is also affected by vertical transport and diffusion. The lower peak perhaps might be due to the contribution of the mesospheric photochemistry. Sometimes horizontal and vertical motion fields in the 70–90 km region might transport atomic oxygen downward producing an increase in the abundance of this constituent in this region. The lifetime of atomic oxygen is of the order of a day
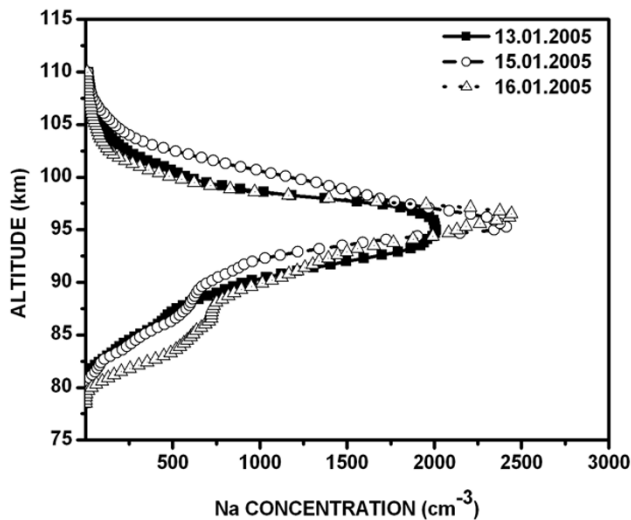
Fig. 5. Mean Na profiles for 13, 15, and 16 January 2005 showing single layer structure.

Fig. 6. Time evolution of Mean Na layer parameters derived from sodium measurements at Gadanki during January 2005. (a) Column abundance (C_0), (b) Centroid position (z_0), and (c) rms layer width (σ_0).

or more in this region so that vertical motions as small as 1–10 cm s^{-1} would be expected to be an important factor in determining the atomic oxygen abundance (Geisler and Dickinson, 1967). Since atomic oxygen is involved in reducing the sodium compounds to atomic sodium, this might be expected to cause a corresponding increase in the atomic Na number density (Clemesha *et al.*, 1995). Thus, the secondary peak of atomic sodium observed could possibly be due to an abrupt increase in atomic oxygen abundance in this region. However, observations and numerical model simulations also indicate that sodium profiles often experience time-dependent large perturbations that are thought to be due to transport associated with gravity waves (Gardner and Voelz, 1987; Clemesha *et al.*, 2001; Xu and Smith, 2003).

We observed a considerable night-to-night variability in the structure of measured mean sodium profiles. Figure 5 shows the average profiles for three subsequent nights 13, 15, 16 January 2006. The profiles show a single peak at 95 km, with a gradual decrease in number density above and below this height. The peak sodium number densities for these profiles appear between 2000 and 2500 cm^{-3}. The profiles show a variation in the peak position of the layer. These profiles were obtained during the time intervals 1903–0600, 2115–0553 and 1957–0555 LT on 13, 15 and 16 January, respectively. It may be mentioned here that the atmospheric waves can cause distortions on the mean sodium layer structure (Gardner and Voelz, 1987; Clemesha *et al.*, 2001). It appears that the structural changes in these profiles may be partly due to perturbations by atmospheric waves such as tides and gravity waves.

3.2 Na layer properties

The structure of the mesospheric Na layer can be characterized by the column abundance (C_o), Centroid height (z_o), and rms layer width (σ_o). The layer parameters are calculated from the different moments of the mesospheric Na layer as given by Gardner *et al.* (1986). Figure 6 shows the average column abundance, centroid position and width of the Na layer for the entire observational period. Figure 6(a)
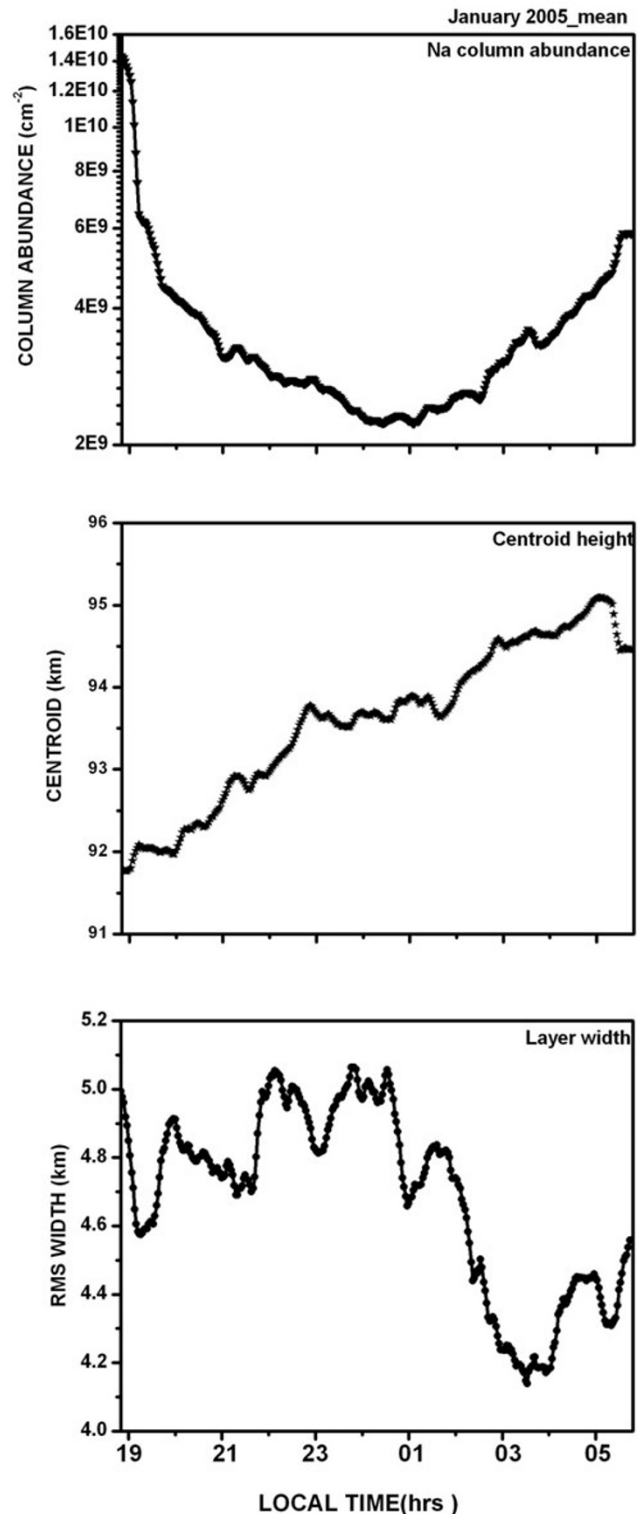
depicts the temporal variation of C_o for January. The total Na content is found to vary between 2×10^9 and 8.9×10^9 atoms cm^{-2}. It shows a variation of more than 400 percent. Simonich *et al.* (1979) found an average nocturnal variation by a factor of 2 in the sodium column abundance at 23°S. Gardner *et al.* (1986) reported more than 200 percent variation in abundance over a midlatitude site. The best part of

the lidar measurements at Gadanki site shows a steady fall in mean column abundance after sunset and a slow raise towards early hours of the day. This means that the total Na content decreases during the night and reaches minimum value during midnight and increases towards sunrise at early hours. The observed nighttime variation could be the manifestation of semidiurnal variation in the sodium layer. This could be perhaps the existence of solar-atmospheric tides in the layer. It is well known that atmospheric tides play an important role in the mesopause region (Chapman and Lindzen, 1970). A number of studies from a low latitude location (Clemesha *et al.,* 1982; Batista *et al.,* 1985; Clemesha *et al.,* 2002) reported the presence of 12-hour oscillation in the sodium layer. Photochemistry in nighttime, dynamics or both may be responsible for the observed variations in the total Na content. Variations in the atomic oxygen number density could be the probable cause for such variations in the sodium content. However, dynamics associated with the layer through horizontal transport may also play a role in the observed variations. Batista *et al.* (1985) concluded that the semi-diurnal oscillations observed in the atmospheric sodium layer at 23°S were mainly induced by atmospheric tides. They were unable to identify any definite chemical effects responsible for such oscillations in the sodium layer. However, States and Gardner (1999) reported from midlatitudes that the variations observed in the sodium layer by them are forced by photochemical effects and not by tidal influenced. The detailed study of these oscillations, from the present data is restricted by the fact that sodium measurements with our lidar were obtained only during nighttime, for which the length of data possible is always less than 11 hours. Hence, it is too early for us to identify the cause for such observed variation in the total Na content. Figure 6(b) presents the mean variation of the centroid (z_o) position of the layer for January. The movement of the sodium layer centroid is a very important parameter to consider for understanding the layer dynamics. The layer mean centroid position alters between 92.9 and 95.2 km. The amplitude of the centroid movement is 2.3 km over the average period of measurement of the night in January. The average rate of variation is around 10 cm s^{-1}, which is typical amplitude of semidiurnal wind reported in the layer (Batista *et al.,* 1985). Figure 6(c) shows the mean variation of rms width of the layer (σ_o) over the mean period for the six nights on which observations were made. The mean rms widths of the layer vary between 4.3 and 4.9 km. The mean layer width has a peak-to-peak variation of about 600 m. It appears that the layer width has an in-phase relation with the sodium column abundance, but an anti-phase relation with the centroid height (Gardner *et al.,* 1986). However, there is a significant wave nature appeared in mean layer width variation. Due to short and long period wave activity such as gravity waves and tides, the structure of the nocturnal layer changes substantially throughout the night. Variations of over 400 percent in abundance, more than 2 km in centroid height, and about 600 m in rms width have been observed within the time span of nocturnal observation.
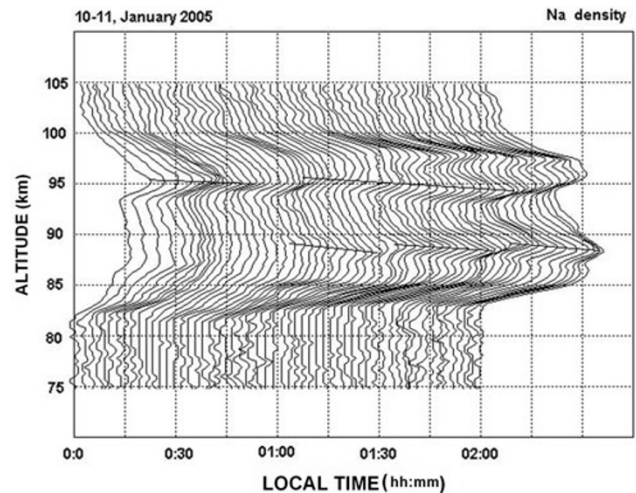

Fig. 7.   Time series of sodium density profiles for 10 January 2005. Inclined lines represent apparent phase propagation.

3.3   Wave parameters

It is generally accepted that the mesospheric Na layer is an excellent tracer of the atmospheric wave motion. The distortions of meteor trails, variations in mesospheric density and temperature profiles, and the study of upper atmospheric disturbances led to the identification of atmospheric buoyancy waves or internal gravity waves (IGWs) as an important feature of dynamics in the upper mesosphere and lower thermosphere (Hines, 1974). These waves are referred to as internal gravity waves because the dominant restoring force on a displaced parcel of air is gravity and the vertical density gradient of the atmosphere allows them to propagate vertically through the medium. Distortions characteristic of the influence of IGWs on winds, density, and temperature give a reliable set of criteria from which to identify their presence. The observed features of meteor trail distortions outlined by Hines (1974) are specific to altitudes between 80 and 110 km. A time series of 2-hour continuous observation of mesospheric Na layer on 10 January 2005 is shown in Fig. 7.

The time resolution of the measurement shown in Fig. 7 is 120 s. The time evolution of perturbations of sodium layer due to gravity wave activity is evident. These perturbations are caused primarily by the vertical displacement of the layer due to vertical component of the gravity wave. Planetary and gravity waves generated in the troposphere propagate into the mesosphere, creating spatial modulations of sodium density profiles as well as temporal variations in sodium column density of the short time periods (Gardner and Shelton, 1985). To identify IGW signatures in the measured Na density, we subtracted the background density from each Na profile. It has been shown that a reasonably accurate model for the unperturbed Na layer (background density) is a Gaussian profile (Gardner and Voelz, 1987). Figure 8 shows the Na density perturbation profiles, which were obtained by background subtraction and normalization. The wave number, period, and amplitude of IGWs can be inferred from Na perturbation profiles (Gardner and Voelz, 1987). A simple Fourier transform of the
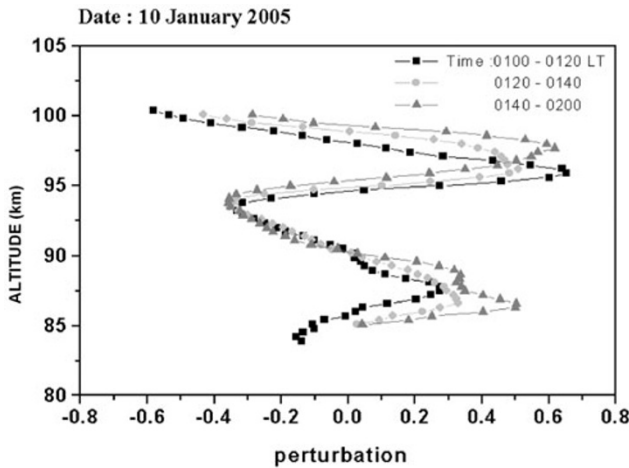
Fig. 8. Perturbation profiles derived from Na profiles for 10 January 2005 averaged for 20 min. during the time interval between 0100 and 0200 LT.
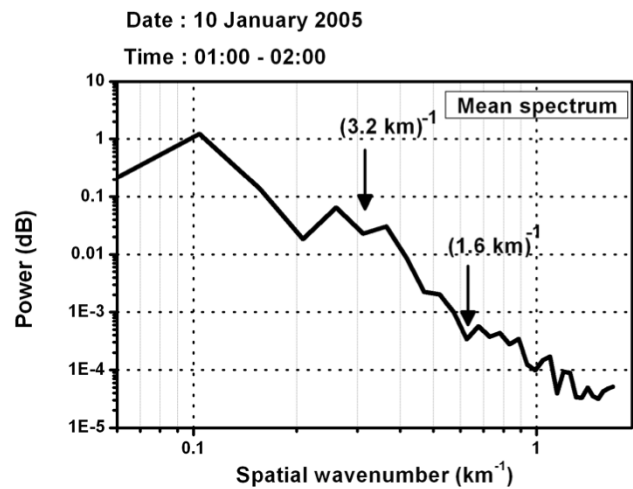

Fig. 9. Power spectrum for the perturbation profiles shown in Fig. 8.

perturbation produces a power spectrum that averaged over a time period. The power spectrum comprised of three terms: the first one indicates a low-frequency lobe in the spectrum. The second term represents the spectral signature of the interactive gravity wave, which is proportional to the square of the wave amplitude. This is shown as a local minimum between two peaks (Gardner and Voelz, 1987). The last term represents the second harmonic component of the gravity wave in action (i.e. generated due to non-linear interaction).

We have applied this analysis in a 20 min. time window, between 0100 LT and 0200 LT, of the 10 January observations. The width of the Na layer sets the maximum vertical wavelength of the wave interacting with the Na layer. In the present study, the maximum vertical wavelength is about 15 km. The altitude resolution decides the minimum wavelength detectable. In this study, the altitude resolution is 300 m. The calculated mean power spectrum is shown in Fig. 9. The feature of the principal wave interacting with the Na layer is evident as the local minimum between the first two peaks on the side of the low frequency part of the spectrum, which indicates the characteristic vertical gravity wave number ($m_o = 0.31$ km^{-1}). This corresponds to approximately 3.2 km wavelength. This wavelength is characteristic wavelength ($\lambda_o = 2\pi/m_o$). The other notch between weaker peaks is at about twice the value of the interactive gravity wave number, which corresponds to 0.62 km^{-1}, generated due to non-linear process. The observations of vertical wavelengths of order 3 km have been observed using lidars, radars and rockets at the mesopause region (Blood *et al.*, 1988; Williams *et al.*, 2006). Usually long period waves such as tides are associated with shorter wavelengths (Williams *et al.*, 2006). The phase velocity of the wave is estimated by dividing the vertical distance the individual wave fronts travel by time between successive observations. The vertical velocity of the wave can be estimated by looking at the motion of the successive peaks, as shown by the inclined lines in Fig. 7. The apparent phase velocity is about 1.0 km h^{-1} or 30 cm s^{-1}, which is consistent with the reported values of the semidiurnal tide in Na

layer (Simonich *et al.*, 1979; Kwon *et al.*, 1987).

3.4   Observation of Sporadic Na layer

An interesting and current topic of interest with the mesospheric Na layer is the sporadic occurrence of thin layers of enhanced number density superposed on the regular background layer. These sporadic layers generate sharp sodium abundance peaks of full width at half maximum (FWHM) typically between several hundred meters and less than a few km thick with number density equal to or greater than twice that of the background Na layer. These layers persist for periods a few minutes to several hours. These sporadic layers appear to be related to the ion layers known as sporadic E, or Es, and for this reason are sometimes referred to as Na$_s$ layers. We have followed the objective method and the criteria given by Miyagawa *et al.* (1999) for identification of Na$_s$ layers in the mesospheric Na layer. Accordingly, in the initial 6 nights of observation, during 54 hours of Na measurements, a total of 4 Na$_s$ layers were observed. The statistical details of the observed Nas layers are listed in Table 3.

On the night of January 10, a sporadic layer was seen between 2200 and 0000 LT and was persisted for about an hour. The altitude of peak number density of the layer was seen at 96.4 km with a strength factor of about 4.5. von Zahn and Hansen (1988) defined a parameter called strength factor to classify the intensity of the sporadic layer. It is the ratio of maximum peak number density of the sporadic layer to the number density of the normal layer at the altitude of the peak of the sporadic layer. Figure 10 shows the altitude/temporal variation of the Na layer during the night of January 11, 2005. On this night, a regular Na layer was seen at the beginning of the experiment as a broad layer extended from 80 to 100 km. At 0232 LT a sporadic layer was formed at about 93 km. Subsequently this sporadic Na layer was observed continuously for almost 2 hours till early morning hours. The peak number density of the sporadic sodium layer is plotted versus time in Fig. 11. The peak of Na layer moved downward from about 96 km to 90 km, with a constant velocity of 24 cm s^{-1}. The altitude of this layer is plotted versus time in Fig. 12.

Table 3. Details of sporadic sodium layer observation.

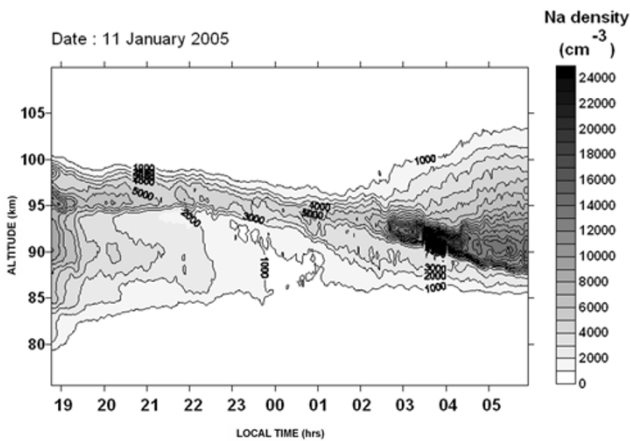| Sl.no	Night observation in January 2005	Period of Na$_s$ layer Observation (LT)	Duration Of SSL (hh:mm)	Time of Max. Density (LT)	Alt. of Max. Density (km)	FWHM (km)	Max.peak Density (cm^{-3})	Strength factor
1	10–11	22.21–23.38	01.17	22.35	96.77	2.1	10296	4.5
2	11–12	02.32–04.32	02.00	03.39	91.68	1.5	29909	7.4
3	15–16	21.15–22.24	01.09	22.00	95.28	1.0	14447	11.9
4	16–17	21.16–00.37	03.21	23.40	95.87	3.0	4466	6.1

Fig. 10. Altitude/Temporal variation of Na density observed on the night of 11 January 2005.
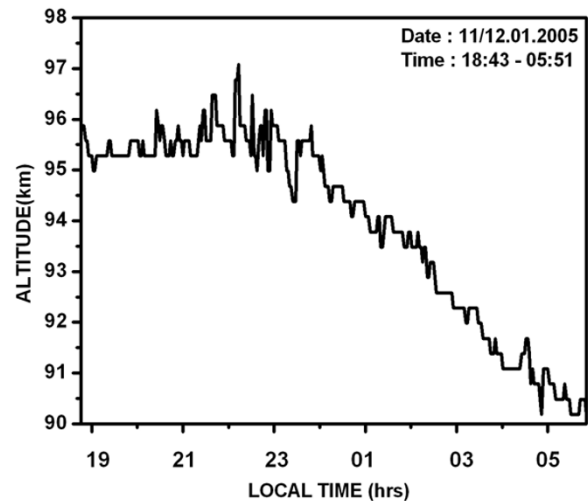

Fig. 12. Temporal variation of the altitude of the dominant sporadic Na layer observed on the night of January 11, 2005, at Gadanki site.
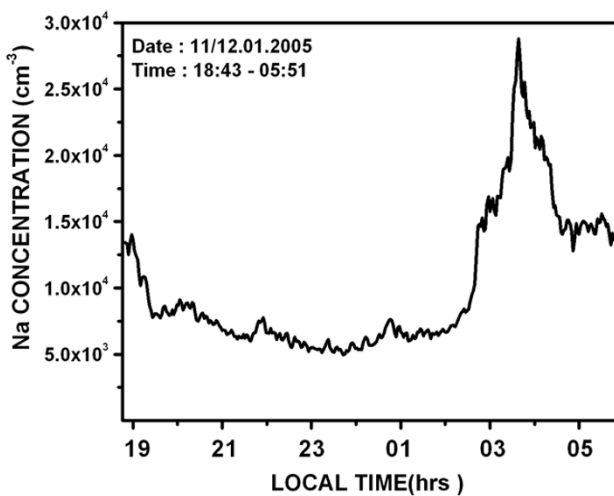

Fig. 11. Temporal variation of the density at the peak of the dominant sporadic Na layer observed on the night of January 11, 2005, at Gadanki site.
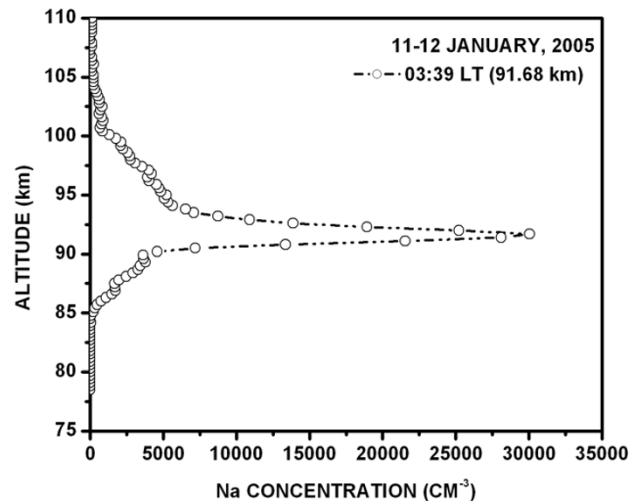

Fig. 13. Peak sporadic layer formation on the background Na layer observed on the night of 11 January, 2005 at 0339 LT.

When the layer descended to an altitude of 91.6 km at 0345 LT, the peak number density reached a maximum of about 29,900 cm^{-3}. In the entire measurement period, the observed Na$_s$ layer has the remarkable peak sodium distribution. Figure 13 shows the peak sporadic sodium layer occurrence on the background Na layer observed on the night of 11 January, 2005 at 0339 LT. On the night of January 15, a strong sporadic layer occurrence at 95 km altitude was observed between 2100 and 2300 LT with a strength factor of about 12 and was observed for about one hour time period.

The peak number density of the sporadic sodium layer is plotted versus time in Fig. 14. Figure 14 shows a narrow and concentrated sodium distribution in to a layer of a few hundred meters thick. On the night of January 16, a relatively long-lived sporadic layer was observed at an altitude of about 96 km. The layer was observed between 2100 and 0100 LT for about 3 hours. The strength factor of the layer was about 6.

Table 4. Details of meteor induced enhanced sodium observation.

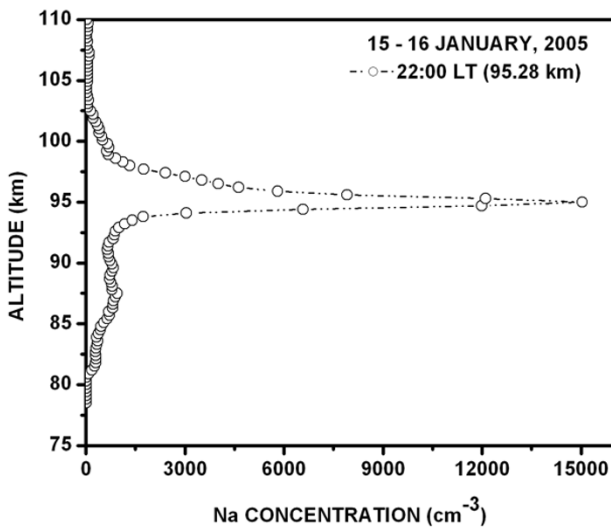| Sl.no	Night observation in January 2005	Period of enhanced Na layer observation (LT)	Duration (hh.mm)	Time of Max Density (LT)	Alt. of Max. Density(km)	FWHM (km)	Max peak Density (cm^{-3})	Density ratio
1	12–13	02.34–02.38	00.04	02.38	95.87	2.50	2680	2.8
2	12–13	03.34–03.38	00.04	03.38	95.58	2.75	2641	2.8
3	12–13	04.05–04.09	00.04	04.09	94.98	2.75	2606	3.2
4	12–13	04.49–04.55	00.06	04.51	93.78	3.00	2469	3.0

Fig. 14. A narrow sporadic layer formation on the background Na layer observed on the night of 15 January, 2005 at 2200 LT.
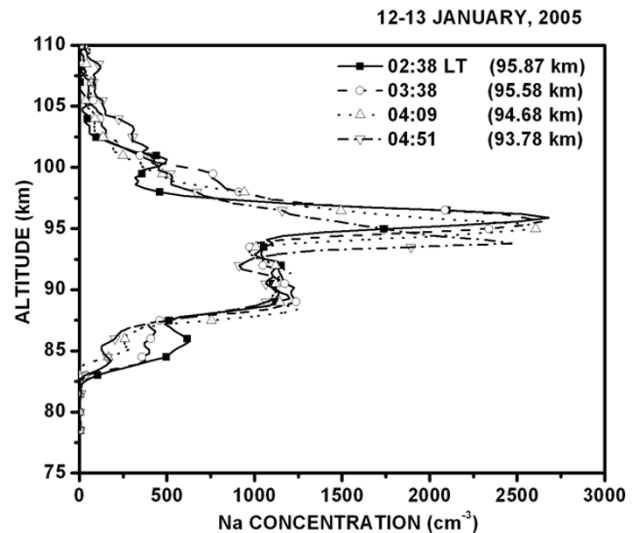

Fig. 15. Observation of narrow sodium layer formations on the night of 12-13 January 2005 due to meteorite ablation.

Lidar observations at low latitudes indicated that the occurrences of sporadic Na layers were usually in the upper part of the normal sodium layers and they often showed a downward motion with time (Batista *et al.,* 1991). Dynamical effects associated with tides, gravity waves and turbulence may also contribute to the formation of sporadic Na layers (Clemesha *et al.,* 1988; Zhou and Mathews, 1995). The sporadic layers in mesospheric Na have been observed at other locations, but their occurrence characteristics seem to vary significantly between the places. Kwon *et al.* (1988) reported at Mauna Kea (20°N) that 16 Na$_s$ layers were seen in 30 h of observations. However, Clemesha *et al.* (1998) observed only 1 layer in 27 h measurements at Alcantara (2°S). The reported observations suggest that the occurrence frequency of Na$_s$ layers decreases as we move from the northern hemisphere low-latitudes towards the southern hemisphere low latitudes. Our observations seem to support the above conclusion, because the observed 8 Na$_s$ layers during nearly 54 h of measurements at Gadanki (13.5°N) fall between the reported observations at Mauna Kea (20°N) and Alcantara (2°S). However, recently Nagasawa and Abo (1995) suggested that the occurrence rate of Nas layers at any location might be related to its magnetic rather than to geographic latitude. Studies on sporadic Na layers have also shown that there is considerable experimental correlation for the occurrences of the mesospheric sporadic Na and sporadic E layers (von Zahn and Hansen, 1988; Cox and Plane, 1998; Clemesha *et al.,* 1999). It is suggested that the

neutralization of the Na ion reservoir in the Es layers is the source of the neutral Na atoms. However, the origin of sporadic sodium layers is still uncertain and involves a more dynamical process (Clemesha, 1995).

3.5 Observation of meteoric induced enhanced Na layer

It is generally believed that the ablation of meteoroids is the only source of metal atoms at the mesopause altitude region. The invention of resonance lidars has made it possible to measure the densities of different metal atoms quantitatively with high vertical and temporal resolution, even inside the trail of an individual meteoroid (Kane and Gardner, 1993; Grime *et al.,* 1999; von Zahn *et al.,* 1999; Drummond *et al.,* 2001, 2002). In our observations, on the night of January 12, four narrow layers of atomic sodium enhancement observed with in a time interval of 3 hours, between 0200 and 0500 LT, as shown in Fig. 15. These layers strength factors appeared in the range between 2 and 3. However, short lifetime, about 4 to 6 minute, is found as the characteristic of these layers. The altitudes of peak number density are appeared between 93 and 96 km. The observational details of the enhanced Na layers are listed in Table 4. We understood that the formation of these narrow layers in short period, such as a few seconds to a few minutes, probably due to advection of meteor trails across the lidar field of view (FOV). In particular, observations during meteor showers such as the prominent Leonids have widely been used to demonstrate the influence of single meteors on the

local metal layer (Hoffner *et al.,* 1999, 2000; Kruschwitz *et al.,* 2001). From such experiments it has become clear that single meteoroids can, in many instances, have large impacts for a short period on the local metal layers.

4.   Conclusion

The first broadband resonance lidar observations of the nighttime sodium layer made on six nights between 10 and 16 January 2005 at Gadanki, a low latitude site, in India have been reported in this paper. During the 6 nights of the initial observational period, nearly 54 hours of Na measurements were obtained. The sodium profile starts to appear around 80 km and rises to a peak close to 95 km and then falls to near zero around 105 km. The topside scale height is always less than 2 km. On three occasions out of a total of six nights of measurements a secondary peak in sodium number density was observed at heights between 87 and 92 km. The mean sodium column abundances were in the range of 2–8.9×10^9 cm^{-2}. The measurements also show the effects of strong tidal perturbations, presumably with a dominant downward propagating semidiurnal tide, but the detailed analysis is not possible due to limited local time coverage. We have seen wave like structures in the sodium layer with typical wavelength of 3.1 km and with downward phase velocities of about 1 km h^{-1}. We have also seen the occurrence of sporadic Na layer over the background mesospheric sodium. A total of 4 sporadic layers were observed during the 54 h of measurement period. Formation and decay of a sporadic layer observed on the night of January 11, 2005, which persisted for a period of about 2 hours, was discussed. The formation of sporadic Na layer developed during downward motion of mesospheric Na layer. Our observations of sporadic Na layer are similar to that reported over other low latitudes. Meteorite induced Na enhancement, which was observed on 12 January 2005, was also discussed.

5.   Future plans

The paper presents the first results from the broadband Na lidar setup at NARL, Gadanki, India. The system has successfully demonstrated the capability to detect waves and other dynamical phenomena such as sporadic layers in the mesopause region. At present, the lidar system configuration allows laser operation in resonant scatter mode only, due to constraints in the laser power distribution. In future, it is planned to operate both the Rayleigh and resonance modes simultaneously. This augmentation helps to understand the wave dynamics in the nocturnal atmosphere covering 30 to 105 km altitude range. Moreover, the extension of Na lidar operation to daytime enables the study of tides in the mesopause region. By narrowing the linewidth of laser, it is also possible to scan the Na D_2 spectrum, from which mesospheric temperatures can be obtained.

References

Alpers, M., T. Blix, S. Kirkwood, D. Krankowsky, F. J. Lubken, L. Lutz, and U. von Zahn, First simultaneous measurements of neutral and ionized iron densities in the upper mesosphere, *J. Geophys. Res.,* **98**, 275–283, 1993.

Batista, P. P., B. R. Clemesha, D. M. Simonich, and V. W. J. H. Kirchhoff, Tidal oscillations in the atmospheric sodium layer, *J. Geophys. Res.,* **90**, 3881–3888, 1985.

Batista, P. P., B. R. Clemesha, and D. M. Simonich, Horizontal structures in sporadic sodium layers at 23°S, *Geophys. Res. Lett.,* **18**, 1027–1030, 1991.

Beatty, T. J., R. L. Collins, C. S. Gardner, C. A. Hostetler, and C. F. Sechrist Jr., Simultaneous radar and lidar observations of sporadic E and Na layers at Arecibo, *Geophys. Res. Lett.,* **16**, 1019–1022, 1989.

Bhavani Kumar, Y., V. Siva Kumar, P. B. Rao, M. Krishnaiah, K. Mizutani, T. Aoki, M. Yasui, and T. Itabe, Middle atmospheric temperature measurements using ground based instrument at a low latitude, *Ind. J. Rad. and Space Phys.,* **29**, 249–257, 2000.

Bhavani Kumar,Y., V. Siva Kumar, A. R. Jain, and P. B. Rao, MST Radar and Polarization lidar observations of tropical cirrus, *Annales Geo. Phy.,* **19**, 873–883, 2001.

Bhavani Kumar, Y., C. Nageswara Raju, and M. Krishnaiah, Indo-Japanese Lidar observations of the Tropical Middle Atmosphere during 1998 and 1999, *Adv. Atm, Sci.,* **23**, 711–725, 2006.

Bhavani Kumar, Y., D. Narayana Rao, M. Sundaramurthy, and M. Krishnaiah, A resonance lidar system for mesospheric sodium measurements, *Journal of Optical Engineering,* 2007 (in press).

Bills, R. E. and C. S. Gardner, Lidar observations of mesospheric Fe and sporadic Fe layers at Urbana, Illinois, *Geophy. Res. Lett.,* **17**, 143–146, 1990.

Blood, S. P., J. D. Mitchell, C. L. Croskey, T. D. Raymund, E. V. Thrane, T. A. Blux, U. P. Hoppe, D. C. Fritts, and F. J. Scmidlin, Studies of high latitude mesospheric turbulence by radar and rocket II: Measurements of small scale turbulence, *J. Atmos. Terr. Pys.,* **50**, 963–976, 1988.

Chapman, S. and R. S. Lindzen, *Atmospheric tides,* 200 pp, D. Reidel Press, Dordrecht, Holland, 1970.

Clemesha, B. R., Sporadic neutral metal layers in the mesosphere and lower thermosphere—Review paper, *J. Atmos. Terr. Phys.,* **57**, 725–736, 1995.

Clemesha, B. R., V. W. J. H. Kirchhoff, D. M. Simonich, and H. Takahashi, Evidence of an extraterrestrial Source for the Mesospheric Sodium Layer, *Geophys. Res. Lett.,* **5**, 873–876, 1978.

Clemesha, B. R., D. M. Simonich, P. P. Batista, and V. W. J. H. Kirchhoff, The diurnal variation of atmospheric sodium, *J. Geophys. Res.,* **87**, 181–186, 1982.

Clemesha, B. R., P. P. Batista, and D. M. Simonich, Concerning of the origin of enhanced sodium layers, *Geophys. Res. Lett.,* **16**, 1267–1270, 1988.

Clemesha, B. R., D. M. Simonich, P. P. Batista, and H. Takahashi, Evidence for a lack of diffusive control of the atmospheric sodium layer, *J. Atmos. Terr. Phys.,* **54**, 355–362, 1992.

Clemesha, B. R., D. M. Simonich, H. Takahasi, S. M. L. Melo, and J. M. C. Plane, Experimental evidence for photochemical control of the atmospheric sodium layer, *J. Geophy. Res.,* **100**, 18,909–18,916, 1995.

Clemesha, B. R., D. M. Simonich, P. P. Batista, and I. S. Batista, Lidar observation of atmospheric sodium at an equatorial location, *J. Atmos. Terr. Phys.,* **60**, 1773–1778, 1998.

Clemesha, B. R., P. P. Batista, and D. M. Simonich, An evaluation of the evidence for ion recombination as a source of sporadic neutral layers in the lower thermosphere, *Adv. Space Res.,* **23**, 547–556, 1999.

Clemesha, B. R., P. P. Batista, and D. M. Simonich, Simultaneous measurements of meteor winds and sporadic sodium layers in the 80–110 km region, *Adv. Space. Res.,* **27**, 1679–1684, 2001.

Clemesha, B. R., P. P. Batista, and D. M. Simonich, Long-term variations in the centroid height of the atmospheric sodium layer, *34th scientific assembly of COSPAR,* Houston, Texas, USA, 10–19 October, 2002.

Cox, R. M. and J. M. C. Plane, An ion-molecule mechanism for the formation of neutral sporadic Na layers, *J. Geophys. Res.,* **103**, 6349–6359, 1998.

Drummond, J. D., B. W. Grime, C. S. Gardner, A. Z. Liu, X. Chu, and T. J. Kane, Observations of persistent Leonid meteor trails: 1. Advection of the "Diamond Ring", *J. Geophys. Res.,* **106**, 21517–21524, 2001.

Drummond, J. D., B. W. Grime, C. S. Gardner, A. Z. Liu, X. Chu, M. C. Kelley, C. Kruschwitz, and T. J. Kane, Observations of persistent Leonid meteor trails 3. The "Glowworm", *J. Geophys. Res.,* **107**, SIA

5-1, doi:10.1029/2001JA000223, 2002.

Fricke, K. H. and U. von Zahn, Mesopause temperatures derived from probing the hyperfine structure of the D$_2$ resonance line of sodium by lidar, *J. Atmos. Terr. Phys.*, **47**, 499–512, 1985.

Gardner, C. S., Sodium resonance fluorescence lidar applications in atmospheric science and astronomy, *IEEEP*, **77**, 408–418, 1989.

Gardner, C. S. and J. D. Shelton, Density response of neutral atmospheric layers to gravity wave perturbations, *J. Geophys. Res.*, **90**, 1745–1754, 1985.

Gardner, C. S. and D. G. Voelz, Lidar studies of the nighttime sodium layer over Urbana, Illinois 2. Gravity waves, *J. Geophys. Res.*, **92**, 4673–4694, 1987.

Gardner, C. S., D. G. Voelz, C. F. Sechrist Jr., and A. C. Segal, Lidar studies of the nighttime sodium layer over Urbana, Illinois, 1. Seasonal and nocturnal variations, *J. Geophys. Res.*, **91**, 13659–13673, 1986.

Gardner, C. S., D. C. Senft, T. J. Beatty, R. E. Bills, and C. A. Hosteller, Rayleigh and sodium lidar techniques for measuring the middle atmosphere density, temperature and wind perturbations and their spectra, *WITS Handbook*, **2**, 148–1187, 1989.

Geisler, J. E. and R. E. Dickinson, Comment on "Upper atmosphere sodium and stratospheric warmings at high latitudes", *J. Atmos. Sci.*, **24**, 720–721, 1967.

Granier, C., J. P. Jegou, and G. Megie, Resonant lidar detection of Ca and Ca + in the upper atmosphere, *Geophy. Res. Lett.*, **12**, 655–658, 1985.

Grime, B. W., T. J. Kane, S. C. Collins, M. C. Kelley, C. A. Kruschwitz, J. S. Friedman, and C. A. Tepley, Meteor trail advection and dispersion: Preliminary lidar observations, *Geophys. Res. Lett.*, **26**, 675–678, 1999.

Hanson, W. B. and J. S. Donaldson, Sodium distribution in the upper atmosphere, *J. Geophys. Res.*, **72**, 5513–5514, 1967.

Hines, C. O., Dynamical heating of the upper atmosphere, *J. Geophys. Res.*, **70**, 177, 1974.

Hoffner, J., U. von Zahn, W. J. McNeil, and E. Murad, The 1996 Leonid shower as studied with a potassium lidar: Observations and inferred meteoroid sizes, *J. Geophys. Res.*, **104**, 2633–2643, 1999.

Hoffner, J., C. Fricke-Begemann, and U. von Zahn, Note on the reaction of the upper atmosphere potassium layer to the 1999 leonid meteor storm, *Earth, Moon and Planets*, **82–83**, 555–564, 2000.

Hunten, D. M., A meteor-ablation model of the sodium and potassium layers, *Geophys. Res. Lett.*, **8**, 369–372, 1981.

Kane, T. J. and C. S. Gardner, Lidar observations of meteoric deposition of mesospheric metals, *Science*, **259**, 1297–1300, 1993.

Kane, T. J., C. S. Gardner, Q. Zhou, J. D. Mathews, and C. A. Tepley, Lidar, radar and airglow observations of a prominent sporadic Na/Sporadic E layer event at Arecibo during AIDA-89, *J. Atmos. Terr. Phys.*, **55**, 499–511, 1993.

Kane, T., B. Grime, S. Franke, E. Kudeki, E. Urbina, M. Kelley, and S. Collins, Joint Observations of Sodium Enhancements and Field-Aligned Ionospheric irregularities, *Geophys. Res. Lett.*, **28**, 1375–1378, 2001.

Kirchhoff, V. W. J. H. and B. R. Clemesha, Atmospheric sodium measurements at 23°S, *J. Atmos. Terr. Phys.*, **35**, 1493–1498, 1973.

Kirchhoff, V. W. J. H., B. R. Clemesha, and D. M. Simonich, The atmospheric neutral sodium layer, 1. Recent modeling compared to measurements, *J. Geophys. Res.*, **66**, 6892–6898, 1981.

Kruschwitz, C. A., M. C. Kelley, C. S. Gardner, G. Swenson, A. Z. Liu, X. Chu, J. D. Drummond, B. W. Grime, W. T. Armstrong, J. M. C. Plane, and P. Jenniskens, Observations of persistent Leonid meteor trails, 2. Photometry and numerical modelling, *J. Geophys. Res.*, **106**, 21 525, (2000JA000174), 2001.

Kwon, K. H., C. S. Gardner, D. C. Senft, F. L. Roesler, and J. Harlander, Daytime lidar measurements of tidal winds in the mesospheric sodium layer at Urbana, Illinois, *J. Geophys. Res.*, **92**, 8781–8786, 1987.

Kwon, K. H., D. C. Senft, and C. S. Gardner, Lidar observations of spo-

radic sodium layers at Mauna Kea Observatory, Hawaii, *J. Geophys. Res.*, **93**, 14199–14208, 1988.

Miyagawa, H., T. Nakamura, T. Tsuda, M. Abo, C. Nagasawa, T. D. Kawahara, K. Kobayashi, T. Kitahara, and A. Nomura, Observations of mesospheric sporadic sodium layers with the MU radar and sodium lidars, *Earth Planets Space*, **51**, 785–797, 1999.

Nagasawa, C. and M. Abo, Lidar observations of a lot of sporadic sodium layer in mid-latitude, *Geophys. Res. Lett.*, **22**, 263–266, 1995.

Nicolet, M., On the molecular scattering in the terrestrial atmosphere: An empirical formula for its calculation in the homosphere, *Planet. Space Sci.*, **32**, 1467–1468, 1984.

Plane, J. M. C., The chemistry of meteoric metals in the Earth's upper atmosphere, *Int. Rev. Phys. Chem.*, **10**, 55, 1991.

Richter, E. S. and C. F. Sechrist Jr, A cluster ion chemistry for the mesospheric sodium layer, *J. Atmos. Terr. Phys.*, **41**, 579–586, 1979.

Richter, E. S., J. R. Rowlett, C. S. Gardner, and C. F. Sechrist Jr., Lidar observation of the mesospheric Na layer over Urbana, Illinois, *J. Atmos. Terr. Phys.*, **43**, 327–337, 1981.

Shibata, Y., C. Nagasawa, M. Abo, T. Maruyama, S. Saito, and T. Nakamura, Lidar observations of sporadic Fe and Na layers in the mesopause region over Equator, *J. Met. Soc. of Japan*, **84**A, 317–325, 2006.

Simonich, D. M., B. R. Clemesha, and V. W. J. H. Kirchhoff, The mesospheric sodium layer at 23°S: Nocturnal and seasonal variations, *J. Geophys. Res.*, **84**, 1543–1550, 1979.

Simonich, D. M. and B. R. Clemesha, Resonant extinction of lidar from the alkali metal layers in the upper atmosphere, *Appl. Optics*, **22**, 1387–1389, 1983.

Slipher, V. M., Emission in the spectrum of the light of the night sky, *Publ. Astron. Soc. Pac.*, **41**, 262–263, 1929.

States, R. J. and C. S. Gardner, Structure of the mesospheric Na layer at 40°N latitude: seasonal and diurnal variations, *J. Geophys. Res.*, **104**, 11783–11798, 1999.

von Zahn, U. and T. L. Hansen, Sudden neutral sodium layers: A strong link to sporadic E layers, *J. Atmos. Terr. Phys.*, **50**, 93–104, 1988.

von Zahn, U., M. Gerding, J. Hoffner, W. J. McNeil, and E. Murad, Fe, Ca, and K atom densities in the trails of Leonids and other meteors: Strong evidence for differential ablation, *Meteorit. Planet. Sci.*, **34**, 1017–1027, 1999.

Williams, B. P., D. C. Fritts, J. D. Vance, C. Y. She, T. Abe, and E. Thrane, Sodium lidar measurements of waves and instabilities near the mesopause region during the DELTA rocket campaign, *Earth Planets Space*, **58**, 1131–1137, 2006.

Williams, B. P., D. C. Fritts, C. Y. She, and R. A. Goldberg, Gravity wave propagation through a large semidiurnal tide and instabilities in the mesosphere and lower thermosphere during the winter 2003 MaCWAVE rocket campaign, *Ann. Geophys.*, **24**, 1199–1208, 2006.

Xu, J. and A. K. Smith, Perturbations of the sodium layer controlled by chemistry or dynamics, *Geophys. Res. Lett.*, **30**(20), 2056–2059, 2003.

Xu, J., A. K. Smith, and R. A. Ma, Numerical study of the effect of gravity wave propagation on minor species distribution in the mesopause region, *J. Geophys. Res.*, **108**, 10.10291/2001JD001570, 2003.

Yi, F., S. Zhang, H. Zeng, Y. He, X. Yue, J. Liu, H. Lv, and D. Xiong, Lidar observations of sporadic Na layers over Wuhan (30.5°N, 114.4°E), *Geophys. Res. Lett.*, **29**, 59.1–59.4, 2002.

Zhou, Q. and J. D. Mathews, Generation of sporadic sodium layers via turbulent heating of the atmosphere, *J. Atmos. Terr. Phys.*, **57**, 1309–1320, 1995.

Y. B. Kumar (e-mail: ypbk@narl.gov.in), P. V. Prasanth, D. N. Rao, M. S. Murthy, and M. Krishnaiah